Direct determination of the band offset in ALD-grown ZnO/hydrogenated amorphous silicon heterojunctions from XPS valence band spectra

L. Korte[a)], R. Rößler, C. Pettenkofer

Helmholtz-Zentrum Berlin, Institute for Silicon Photovoltaics, Kekuléstrasse 5, 12489 Berlin, Germany

The chemical composition and band alignment at the heterointerface between ALD-grown zinc oxide (ZnO) and hydrogenated amorphous silicon (a-Si:H) is investigated using monochromatized X-ray photoelectron spectroscopy. A new approach for obtaining the valence band offset ΔE_V is developed, which consists in fitting the valence band (VB) spectrum obtained for a-Si:H with a thin ZnO overlayer as the sum of experimentally obtained VB spectra of a bulk a-Si:H film and a thick ZnO film. This approach allows obtaining $\Delta E_V = 2.71 \pm 0.15$ eV with a minimum of assumptions, and also yields information on the change in band bending of both substrate and ZnO film. The band offset results are compared to values obtained using the usual approach of comparing valence band edge-to-core level energy differences, $\Delta E_{B,CL} - \Delta E_{B,VB}$.

Furthermore, a theoretical value for the VB offset is calculated from the concept of charge neutrality level line-up, using literature data for the CNLs and the experimentally determined ZnO/a-Si:H interface dipole. The thus obtained value of $\Delta E_V^{CNL} = 2.65 \pm 0.3$ eV agrees well with the experimental ΔE_V.

I. Introduction

Zinc oxide, typically doped with aluminum (ZnO:Al), is a widely used transparent conductive oxide (TCO) material. In the field of silicon photovoltaics it is used as contact layer in "classical" amorphous or amorphous/microcrystalline solar cells [1,2], in wafer-based high efficiency heterojunction cells [3] and also in novel device concepts such as polycrystalline silicon thin film cells on glass [4,5]. Typically, in such devices junctions are formed between ZnO:Al or other degenerately doped TCOs and hydrogenated amorphous (a-Si:H) or microcrystalline, (µc-Si) films. In TCO/a-Si:H/c-Si structures, it has been shown, that the interplay of band line-up at the TCO/a-Si:H interface and doping of the a-Si:H films has a significant influence on the band bending in the crystalline wafer [3], which impacts device properties such as the solar cell's fill factor. However, while for ZnO:Al/µc-Si and ZnO:Al/a-SiO$_x$:H, the band alignment at the heterointerfaces has been studied recently using photoelectron spectroscopy (PES) [6], to our knowledge, no such data exists for the ZnO/a-Si:H interface. Note, that the incorporation of oxygen in a-Si:H leads to an increasing band gap, thus

---

[a)] Author to whom correspondence should be addressed. Electronic mail: korte@helmholtz-berlin.de.

variations in the band offsets. Therefore, it is not straightforward to extrapolate the results of Ref. [6] to the ZnO/a-Si:H case.

In studies such as Gerlach's [6], band offsets are usually obtained from the comparison of valence band edge-to-core level energy differences, $\Delta E_{B,CL} - \Delta E_{B,VB}$, in heterojunctions formed between the substrate and an overlayer that is thinner than the PES information depth [7]. This technique requires to measure both valence band (VB) and core level (CL) spectra and is prone to systematic errors e.g. if changes in the material's stoichiometry invalidate the assumption of fixed CL-to-VB edge distances. In the present paper, we suggest an alternative approach to analyzing such heterojunctions: The spectrum obtained from the substrate-with-thin-overlayer sample is described as the sum of weighted and shifted VB spectra measured on thick films of the involved materials. In this way, parameters such as band offsets and the change in band bending can be obtained easily and with a minimum of assumptions. In order to investigate the initial growth stages and the band lineup at the ZnO/a-Si:H interface, thin films of ZnO were grown on a-Si:H by atomic layer deposition (ALD). To avoid any influence of surface contamination/adsorbates, they were transferred under UHV conditions (p < 10^{-9} mbar) and characterized using monochromatized XPS.

II.   Experimental details

Nominally intrinsic amorphous silicon, (i)a-Si:H, films were deposited onto a ~3 Ωcm (n)c-Si wafer in a conventional 13.56 MHz PECVD system [8] with a base pressure of 10^{-7} mbar using the parameters substrate temperature: 170°C; deposition pressure: 0.5 mbar; RF power: 10 W, SiH_4 gas flow: 10 sccm. An a-Si:H film thickness of 20 nm was chosen in order to avoid any contribution of the c-Si substrate to the PES signal. After deposition, the sample was immediately transferred into a UHV system (base pressure < 10^{-9} mbar) described elsewhere [9]. The absence of surface adsorbates or oxidation during the sample transfer was confirmed using XPS. ZnO was deposited in a home-made set-up from the precursor gases $Zn(C_2H_5)_2$ and H_2O. Cycle times were 400 ms for $Zn(C_2H_5)_2$ and 200 ms for H_2O, with intermediate purging and pump-down steps of 25 ms and 20 s duration, respectively. The chamber pressure was in the 10^{-1} mbar range during both the $Zn(C_2H_5)_2$ and the H_2O cycle. In order to avoid changes in the a-Si:H due to unwanted thermal annealing, the sample

temperature was set to 190°C, i.e. slightly below the center temperature of 210°C of the constant ALD growth rate window established in a previous study [9].

After a few ALD cycles, the sample was transferred in UHV to a separate photoelectron spectroscopy chamber where monochromatized XPS (MXPS) measurements were carried out using Al K_α radiation with a SPECS FOCUS 500 X-ray monochromator for excitation at an energy of $h\nu = 1486.74$ eV and a PHOIBOS 150 hemispherical energy analyzer. The energy resolution was set to 250 meV. Additional UPS measurements were carried out using He I ($h\nu = 21.2$ eV) excitation. The sample was then transferred back to the ALD chamber, and the sequence of ALD and subsequent PES was repeated. Thus, all data for different ZnO thicknesses reported in the following were obtained from the same sample. The reproducibility of the process was verified on additional a-Si:H samples as well as previously on c-Si [9] and also on $CuInSe_2$ substrates [10].

The band gaps of a-Si:H and ZnO were determined from spectral ellipsometry (SE) in the wavelength range $\lambda = 300\ldots850$ nm and $300\ldots1200$ nm, respectively, using a SENTECH SENresearch SE 850 spectral ellipsometer.

III. Results and discussion

A. Formation of the ZnO/a-Si:H interface

Fig. 1 shows the Si 2p core level emission for the a-Si:H/c-Si substrate and the ZnO/a-Si:H/c-Si structure after 5 ZnO ALD cycles as well as the O 1s core levels after 5 and 24 ALD cycles. The double peak structure of the Si 2p spin-orbit splitting (fitted peak positions: 99.6 eV and 100.2 eV for the Si 2p 3/2 and 1/2 peak, respectively) is not fully resolved for the a-Si:H substrate spectrum (Fig. 1a), although the energy resolution of the MXPS setup is sufficient to resolve the peaks for crystalline silicon samples. This is the usual observation made in high resolution XPS of a-Si:H: the line broadening reflects the disorder in the amorphous Si film. A weak shoulder is due to Si[1+] oxidation states; no contributions from higher oxide states are observed. This confirms the absence of a-Si:H surface contaminations prior to ZnO deposition.

For the thinnest ZnO film (5 ALD cycles, ~1.1 nm ZnO), minor additional contributions from the Si[2+] and Si[3+] states can be detected, at a level of ~3% relative to the area of the main peak. This correlates

with the peaks found in the O 1s spectra. These contributions decrease below the detection limit for higher ZnO thicknesses, since also the overall Si 2p peak area decreases (see below).

In both O 1s spectra, the O_2^- peak from stoichiometric ZnO in the wurtzite phase at 531.1 eV is dominant. Additional peaks with lower intensity can be assigned to Zn-OH (OH^- peak) and SiO_x phases in the sample. Clearly, the contribution of a 4th peak has to be assumed in order to obtain a proper fit to the data. Based on previous studies [9] and the chosen growth conditions (low growth temperature; H_2O as oxygen precursor; H_2O is always the final ALD cycle prior to sample transfer to the PES chamber), we relate this peak to adsorbed water on the ZnO film. In order to verify these assignments, peak intensities were cross-check between different core levels: e.g. for the SiO_x peak, a corresponding intensity was found in the Si 2p oxide peak.
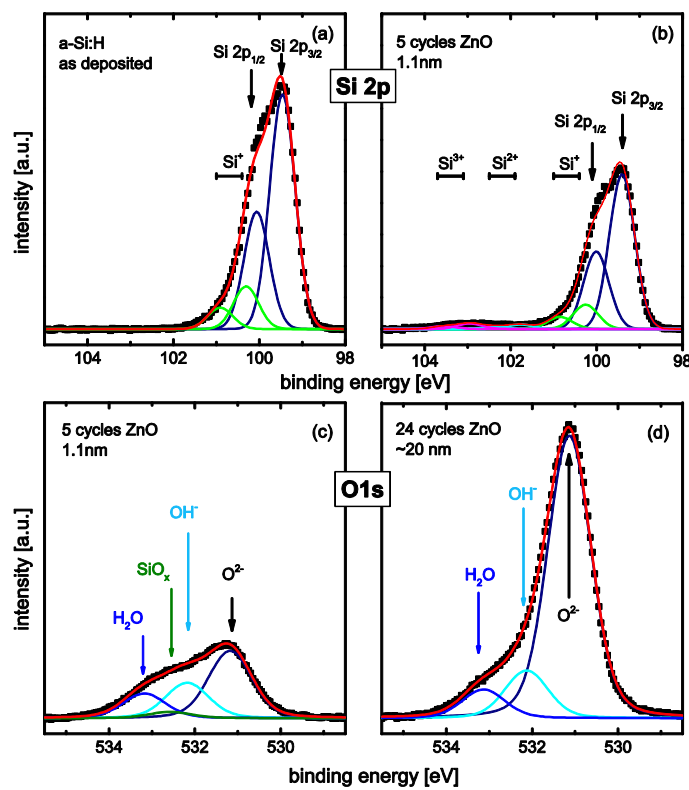

Figure 1: Si 2p and O 1s core level spectra as measured (linear background subtracted) with Al K_α MXPS (a) before, (b,c) after 5 and (d) 24 ALD ZnO deposition cycles. Within the same row, the scaling of the ordinates is identical, i.e. peak heights can be compared directly. In the upper row, the positions of the spin-orbit split Si 2p main peak and of the suboxides $Si^+...Si^{3+}$ are marked. In the lower row, the positions of the main O^{2-} peak stemming from O in Zn-O in the wurtzite structure as

well as of OH⁻ (Zn-OH), H_2O adsorbed on the sample surface and SiO_x at the ZnO/a-Si:H interface are indicated.

With increasing number of ALD cycles (increasing ZnO thickness), the stoichiometric O^{2-} peak becomes more pronounced. The intensities of the OH⁻ and H_2O peaks are unchanged, indicating that they must be related to contributions from the surface or near-surface region of the growing ZnO layer. From the peak ratios, a composition of [Zn-OH]:[Zn-O] ~ 15-20% is estimated for the near-surface region of the "bulk" – about 20 nm thick – ZnO film (Fig. 1d). In fact, using ALD and a low growth temperature makes it unlikely that the stoichiometry in the bulk of the ZnO film will change (namely, that the hydroxide will be converted into stoichiometric ZnO). Thus, it can be surmised that the Zn-OH phase is indeed located entirely on the free surface of the ZnO film, where in addition adsorbed H_2O is present, while the bulk consists of stoichiometric material.

The fit to the O1s core level of the thinnest film (Fig. 1c) shows that the intensity of the SiO_x peak is at the detection limit. This is in contrast to previous studies of sputtered ZnO:Al [11], where SiO_x and an additional peak assigned to a Zn_2SiO_4 silicate phase were dominant in O 1s spectra of similarly thin films and significant oxidation of the Si/ZnO interface was found ([SiO_x]:[Zn-OH] ~ 1:1 for 1.7 nm ZnO). We thus conclude, that the ALD-ZnO/Si interface is abrupt and free of additional mixing phases, in contrast to the ill-defined sputtered ZnO/Si interface, and similar to the MOMBE-grown ZnO films on c-Si(111):H also discussed in the publication by Meier & Pettenkofer [11]. The abruptness of the interface is further verified by high resolution TEM micrographs (not shown here).

B.   ZnO film growth mode and film thickness

Assuming an exponential damping of the substrate core level emission by the ZnO overlayer, the peak area ratio of core levels from the Si substrate and the growing ZnO film as shown in Fig. 2a can be used to calculate the ZnO film thickness d_{ZnO}, using

$$I_{Si2p}(d_{ZnO}) = I_{0,Si2p} \exp(-d_{ZnO}/\lambda_{imfp}), \tag{1}$$

where λ_{imfp} is the inelastic mean free path in ZnO of the Si 2p photoelectrons stemming from the substrate, I_{Si2p} the integrated Si 2p core level emission intensity and $I_{0,Si2p}$ this emission intensity without ZnO overlayer. Fig. 2b shows the ZnO film thickness vs. number of ALD cycles thus

obtained. The linear increase of ZnO thickness with ALD cycle no. indicates a layer-by-layer growth of the film after ~5 cycles, with a rate of ~1 nm/cycle. The offset (extrapolation of the linear behavior not crossing the origin) is most likely due to a nucleation phase as a first growth stage, where steric hindrance of the precursor molecules on the surface inhibits the growth of a full monolayer of the film per cycle, because the areal density of reaction sites for the $Zn(C_2H_5)_2$ precursor is different on –OH terminated a-Si:H as compared to –OH terminated ZnO.
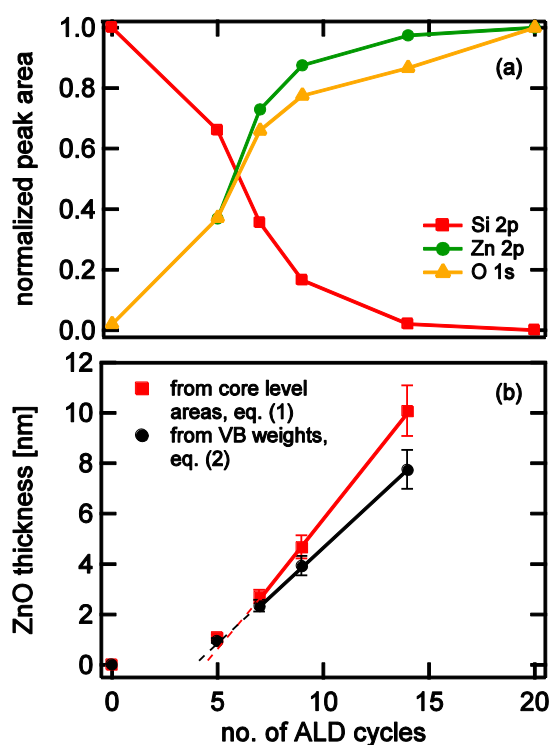

Figure 2: (a) Normalized peak areas of the Si 2p core level (a-Si:H substrate) and of the Zn 2p and O 1s levels (ALD ZnO film). (b) ZnO film thickness vs. number of ZnO ALD cycles, as calculated from the Si 2p core level peak areas (■) and from the scaling factors C_{aSi}, C_{ZnO} obtained from fitting eq. (2) to the XPS valence band spectra (●).

C. ZnO/a-Si:H band offset

Moving on to the main subject of the present paper, i.e. the determination of the band offset in the ALD-ZnO/a-Si:H heterojunction, we show in Fig. 3 MXPS data from the valence band of the ZnO/a-Si:H stacks. Plotted against a linear ordinate, the increase of the Zn 3d core level emission at a binding energy of $11.1 - 11.2$ eV and the ZnO valence band edge at $3.6 - 3.7$ eV with increasing ZnO film

thickness are clearly identifiable. More information becomes visible when the same data is plotted against a logarithmic ordinate (Fig. 3b): Now, an additional contribution from the a-Si:H substrate's valence band can be discerned in the spectra. Note, that it is essential to use monochromatized XPS in a state-of-the-art XPS set-up for this study, for two reasons: first, to provide an increased energy resolution, which is essential for obtaining the valence band edges of ZnO and, especially, a-Si:H from the VB spectra, cf. Fig. 4. Second, to suppress the high energy Al K_α satellite lines present in un-monochromatized XPS: These satellite lines give rise to (low intensity) replicas of the valence band spectra that are shifted to higher energies and thus obscure the true shape of the VB edges as well as the low-intensity emission from the a-Si:H substrate in the ZnO/a-Si:H stacks.
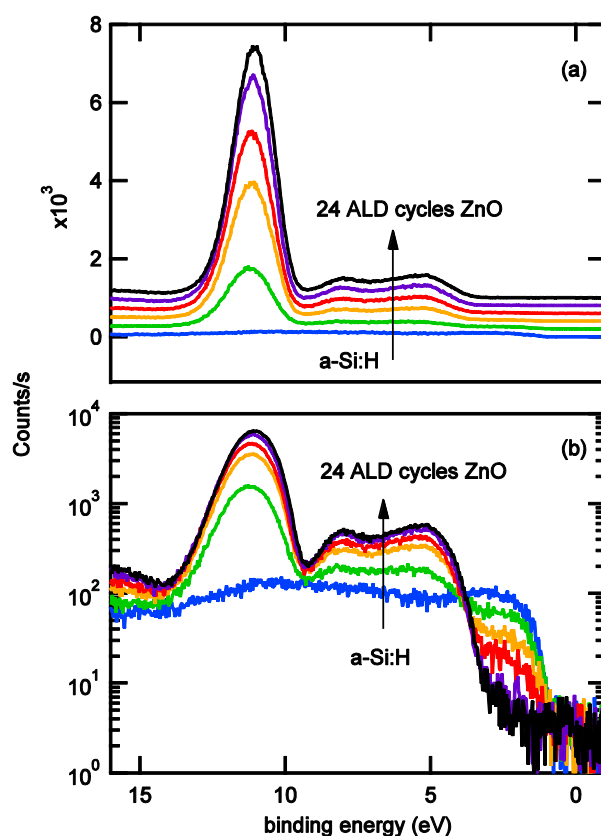

Figure 3: XPS valence band spectra for the a-Si:H substrate and the series of 5-24 ALD cycles of ZnO. (a) linear, (b) logarithmic scale. For better visibility, the spectra in (a) are slightly offset.
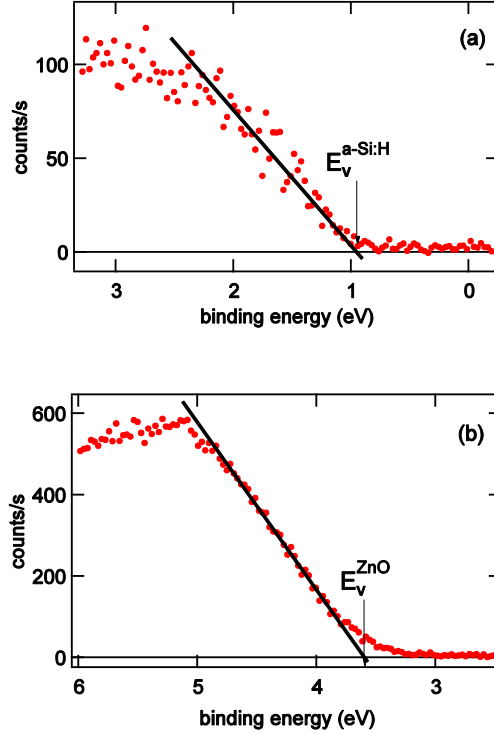
Figure 4: Valence band edges of (a) 20 nm (i)aSi:H as-deposited on c-Si and (b) the same sample after 24 ALD cycles of ZnO deposition. Valence band edge positions $E_V^{\text{a-Si:H}}$ and E_V^{ZnO} as determined from linear fits are marked in the plots.

We start by determining the valence band edges of the (i)a-Si:H substrate and the thick intrinsic ALD-ZnO film as usual from the intercept between a linear fit to the leading edge of the valence band spectrum in the measured spectra and the abscissa (counts/s = 0), cf. Fig. 4. The fits yield $E_V - E_F =$ 1.00±0.06 eV and 3.60±0.08 eV for a-Si:H and ZnO after 24 ALD cycles, respectively. This is consistent with band edge positions obtained in the same way from conventional UPS (0.90 and 3.52 eV, respectively). Note, that the quoted 1σ errors are those obtained from the fit. They do not include systematic errors due to the measurement procedure, calibration of the energy scale and definition of band edges. For the determination of the ZnO/a-Si:H valence band offsets ΔE_V, the first two of these cancel out, cf. Eq. (2). We estimate the remaining systematic error for the determination of ΔE_V to ~150 meV. The main source of error is that is generally difficult to define a band edge energy in amorphous semiconductors: Instead of a sharp band edge, the density of states tails off into the band gap. For electrons and holes in the semiconductor, this gives rise to a mobility band edge, i.e.

a demarcation energy between extended (conduction) states and localized (band tail) states in the so-called Urbach tail. For the case of a-Si:H, we have shown previously based on a comparison between near-UV photoelectron valence band spectra and electrical measurements of the activation energy, that the valence band mobility edge $E_{V\mu}^{aSiH}$ is located in such spectra at the transition energy between the linear band edge and the exponential Urbach tail [12,13]. For the present case, this yields $E_{V\mu}^{aSiH}$ ~ 0.94 eV, i.e 100 meV below E_V^{aSiH}. To stay consistent with the usual XPS/UPS VB edge determination procedure in the literature, we use in the following the $(E_V - E_F)_{aSiH}$ obtained from the linear extrapolation.

The monochromatized XPS provides a very good signal-to-noise ratio, due to the absence of background and satellites in the emission of the XPS source, as discussed above: A dynamic range of almost four orders of magnitude in the usable VB spectrum allows to monitor the emission from the a-Si:H substrate's valence band up to a ZnO overlayer thickness of about 8-10nm (14 ALD cycles).
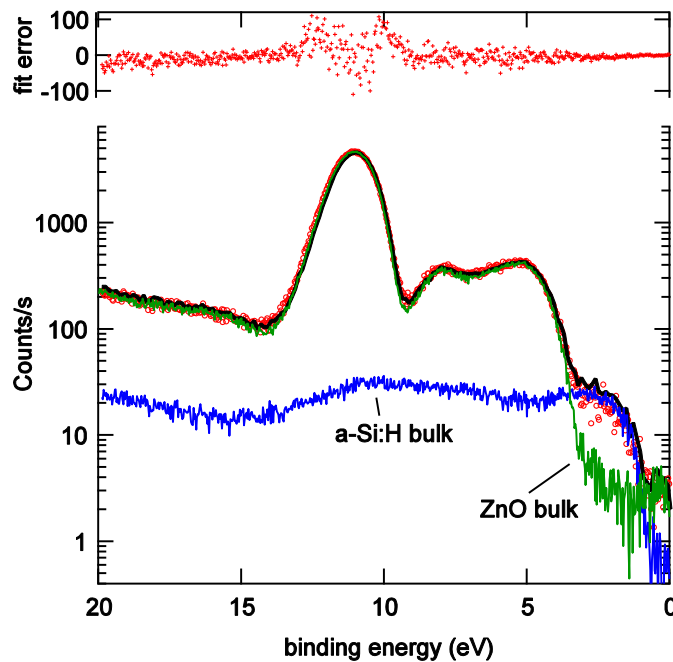
Figure 5: Valence band spectrum of the ALD ZnO/2nm (i)a-Si:H/c-Si layer stack after 9 ALD cycles (○). The black curve is fitted to this spectrum. It is calculated as the sum of two scaled and shifted "bulk" reference spectra: An a-Si:H substrate spectrum (raw data, scaled and shifted: blue) and a ZnO "bulk" (24 ALD cycles) spectrum (raw data, scaled and shifted: green). The scaling factors and energy offsets, cf. eq. 2, are the free parameters used for fitting. The residual error of the fit is shown above

the main graph.

We find that under these conditions, the VB spectra of the intermediate ZnO film thicknesses (5-14 ALD cycles) can be modeled as the superposition of the initial a-Si:H VB spectrum with that of a thick ALD-ZnO ("bulk") film: Fig. 5 shows an exemplary fit of the XPS VB data from a ZnO/a-Si:H sample after 9 ALD cycles. The model spectrum used for the fit is based on the a-Si:H XPS VB spectrum and the ZnO XPS VB spectrum after 24 ALD cycles and is calculated as

$$Cps(E) = C_{aSi}\, Cps_{aSi}(E+\Delta E_{aSi}) + C_{ZnO}\, Cps_{ZnO}(E+\Delta E_{ZnO}), \tag{2}$$

where Cps_i is the experimentally obtained XPS count rate from the VB spectrum of the respective "bulk" films, i.e. of the as-deposited a-Si:H film and the ZnO after 24 ALD cycles. "Bulk" means in the present context, that the film thickness is greater than the information depth ($\sim \lambda_{imfp}$) of the VB XPS, so that the spectrum contains no contributions from the substrate. C_i scale the contributions of the a-Si:H and ZnO bulk spectra to the sum spectrum, and the ΔE_i shift those spectra along the binding energy ($E_F \equiv 0$) axis. The fit is carried out using a Levenberg-Marquardt least squares algorithm, all four parameters C_i, ΔE_i are used as free parameters. As is evident also from the residual error ($Cps_{measured} - Cps_{fit}$) shown in Fig. 5, an excellent fit is obtained by this procedure. The only remaining discrepancy between the fitted model data and the measurement occurs in the region $E_{bind} \sim$ 10…13 eV: the Zn 3d peak width is slightly increased for the thin ZnO film, as compared to the ZnO bulk spectrum. This symmetric broadening (cf. the symmetric "wings" in the residual error) is likely due to an increased disorder and/or lattice stress in the ZnO film close to the heterointerface. Note, that the observation of a symmetric residual error around the Zn 3d peak location is consistent with the picture that OH⁻ is present only at the film surface, but not incorporated into the ZnO bulk: Variations in the OH⁻ – related contribution to the Zn 3d peak between the "bulk" spectrum and the film after 9 ALD cycles would lead to an asymmetry in the residual error. Furthermore, we point out that it was not necessary to take into account the effects of inelastic scattering of photoelectrons in Eq. (2): Such inelastic scattering redistributes the photoelectron count rate to higher binding energy (e.g. [14,15]), i.e. away from the leading edge of the valence band. This effect would be most pronounced for photoelectrons coming from the a-Si:H bulk, or from deep-lying parts of the ZnO film, and would lead

to peak asymmetries and a distorted a-Si:H valence band spectrum. However, no such effects were visible in the MXPS data, probably because the inelastic underground in the a-Si:H VB spectrum is obscured by the rapidly increasing contribution from the ZnO overlayer's VB (cf. Fig. 5, compare the scaled a-Si:H spectrum to that of the ZnO bulk). It should also be noted that for less well-defined heterointerfaces such as the sputtered ZnO:Al/c-Si interface [11], additional contributions from the mixed phases at the interface could be expected in the valence band region. The fact that no such contributions have to be invoked in the fitting process is additional proof for an abrupt interface in our ZnO/a-Si:H samples.

Under the same assumptions as above (but using the appropriate ZnO λ_{imfp} of 2.72 nm corresponding to an average photoelectron kinetic energy of 1480 eV), eq. (1) can be used to calculate the ZnO film thickness, using the ratio C_{aSi}/C_{ZnO} instead of the intensity ratios $I_{aSi}/I_{0,aSi}$. The result is plotted in Fig. 2b, and is similar to the thickness obtained from the core level intensities, albeit with a slightly smaller growth rate (~0.8 nm/ALD cycle). This discrepancy can be explained at least partially by the not precisely known λ_{imfp}s (error bars in the graph).

Taking the values ΔE_{aSi}, ΔE_{ZnO} from the fit of eq. (2), the positions of the valence band maxima of a-Si:H and ZnO in the spectra for 5…14 ALD cycles can be calculated from the initial values E_V-E_F reported above as $(E_{V,i} - E_F)_{cycle} = (E_{V,i}-E_F) + \Delta E_i$. The result of this procedure is shown in Fig. 6, together with VB maxima positions for the same samples calculated with the standard procedure of reduced XPS core level binding energies [7]. In the latter case, the distance of the valence band edge from the core level(s) of the materials forming a heterojunction – the so-called reduced binding energies $E_{B,CL} - E_{B,VB}$ – are computed from bulk spectra, and the relative shift of substrate and overlayer core level positions for thin overlayers is then taken as the change of band offset in the heterojunction. Note, that this approach relies on the assumption that the distance between core level(s) and valence band edge is fixed in all investigated samples. Especially in heterojunctions where chemical reactions of the two materials forming the interface are likely, this assumption can be questioned. For the evaluation based on the direct measurement of XPS VB spectra as proposed here, such an assumption is not necessary. Indeed, the valence band edges calculated from the reduced binding energies of the ZnO-related core levels Zn 3d, Zn 2p and O 1s differ slightly for the thinnest

films (5, 7 and 9 ALD cycles), where variations in ZnO film properties are most likely due to the proximity of the a-Si:H interface. Taking the slightly broadened Zn 3d core level (Fig. 5) into account, it can be speculated that an increased disorder in the ZnO film close to the interface might be the reason for both findings.
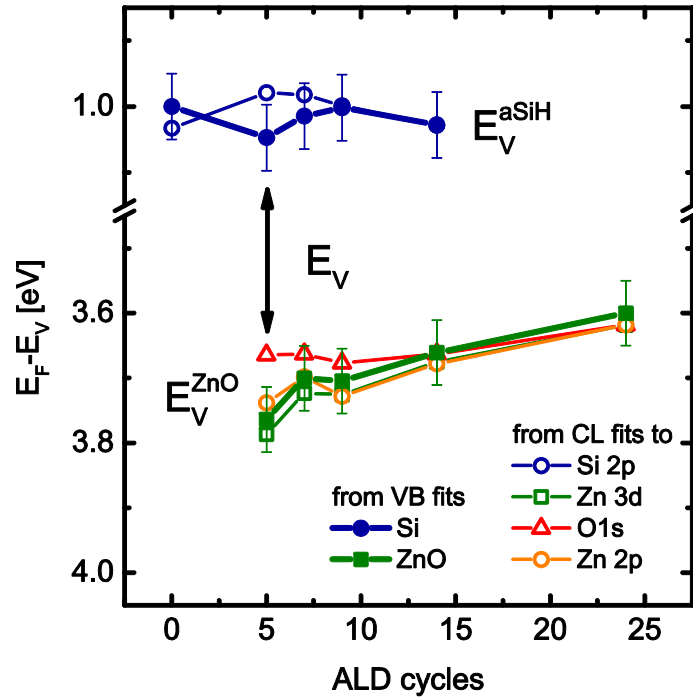
Figure 6: Positions of the valence band maxima of the a-Si:H substrate and ZnO film. The ZnO/a-Si:H valence band offset ΔE_V is given by the difference between these energies.

In Fig. 6, both the direct and the reduced band offset method indicate within experimental error a constant position of the a-Si:H band edge upon initial ZnO deposition as well as for increasing ZnO thickness. Thus, no (additional) band bending is induced in the a-Si:H film when the junction with the ALD-ZnO is formed. Indeed, it is probable that no band bending is present also in the a-Si:H film prior to ZnO deposition: Evaluating spectral ellipsometry (SE) data ($\lambda = 300\ldots850$ nm) with a Tauc-Lorentz model [16], we obtain a band gap of 1.72 eV for our a-Si:H films. Nominally undoped a-Si:H is slightly n-type, i.e. the bulk Fermi level is expected to lie above midgap, $E_g/2 = 0.86$ eV. Indeed, based on near-UV photoelectron yield spectroscopy in the constant final state mode (CFSYS) we have

reported values around 1.1 eV for $E_F - E_{V\mu}$ in intrinsic films deposited in the same PECVD system as used here [12]. Thus, the measured $E_{V\mu}^{aSiH} - E_F \sim 1.00$ eV is compatible with a surface band bending of 140 meV at most.

The situation is different for the ZnO film: With increasing film thickness, $E_{V,ZnO} - E_F$ decreases by ~ 200 meV over the investigated range of ZnO thicknesses. Thus, a slight band bending is probably present in the nominally undoped ZnO film. Note, that in principle the measured trend could also be explained by a film thickness dependent variation of the ZnO band gap and concomitant shift of the valence band edge towards the Fermi level. However, since we see no change in the ZnO XPS data except the discussed slight change in Zn 3d peak width, such a pronounced change of the valence band structure appears unlikely.

Spectral ellipsometry data ($\lambda = 300\dots1200$ nm) measured on the 24 ALD cycles ZnO/a-Si:H stack was fitted to obtain the ZnO band gap $E_{g,ZnO}$, and film thickness d_{ZnO}. For the ZnO film, a model proposed by Leng [17] was used to describe the band edge absorption in the UV. For the free carrier absorption in the infrared, an extended Drude model was used [18]. The fit yields d_{ZnO}, = 22.2 nm, close to the value of $d_{ZnO} \sim 20$ nm for 24 ALD cycles ZnO as obtained by linear extrapolation of the core level peak area data shown in Fig. 2(b). However, note that the same extrapolation for the VB weights (Eq. (2)) gives only ~16 nm. In the SE model, it was sufficient to assume a stack consisting of only ZnO bulk/a-Si:H bulk on c-Si, i.e. no interfacial or surface layers with differing composition had to be assumed. This indicates, again, a homogenous growth of ALD ZnO on the a-Si:H film surface. We found that the SE fit was not very sensitive to the ZnO band gap: values in the range $E_{g,ZnO} = 3.3\dots3.5$ eV led to similarly good fits. For the band diagram in Fig. 7 we adopt a mean value of 3.4 eV. Note, that similarly low values have been reported in the literature for sputtered undoped ZnO films, e.g. [19].

Taking the difference between the ZnO and a-Si:H VB edge positions for the thinnest ZnO film (5 ALD cycles), we obtain an ALD-ZnO/a-Si:H valence band offset ΔE_V of 2.71±0.15 eV and, using the SE band gap of 3.4eV, a conduction band offset ΔE_C of 1.03±0.3 eV. The uncertainty of these values is dominated by systematic errors such as the definition of the a-Si:H band edge and SE optical band gaps, as discussed already above. The ZnO and a-Si:H work functions are obtained from UPS 21.2 eV

measurements on the a-Si:H substrate and on the thinnest ZnO film: $\Phi_{aSiH} = 4.40\pm0.01$ eV and $\Phi_{ZnO} = 3.64\pm0.01$ eV, respectively. From these values, we obtain the a-Si:H/c-Si interface dipole, $\Delta = \Phi_{aSiH} - \Phi_{ZnO} - \delta q\phi_{s,aSi} = 0.72\pm0.1$ eV, where $\delta q\phi_{s,aSi} = 0.04\pm0.1$ eV is the additional surface band bending induced in the a-Si:H upon deposition. The latter value is calculated from the difference in a-Si:H VB edge positions prior to and after 5 ALD cycles ZnO deposition (cf. Fig. 6).

Putting these values together, the ALD-ZnO/a-Si:H heterojunction band diagram as sketched in Fig. 7 for the sample after 14 ALD cycles is obtained. Note, that these results place the Fermi level in the ZnO conduction band, i.e. the ZnO is degenerate n-type. This is an unexpected result, since the ALD-ZnO film is nominally undoped. The slight band bending with increasing ZnO thickness (~100 meV for the 14 ALD cycles, Fig.6; ~200 meV after 24 ALD cycles) observed as a shift of the ZnO core level positions and VB edge indicates that charge equilibration at the ZnO/a-Si:H interface plays a role. Indeed, since Debye screening lengths of hundreds of nm have been reported for undoped ZnO [20], it is likely that even in the thickest ZnO film investigated here, the Fermi level has not yet reached its bulk equilibrium value. Further investigations are planned to clarify this point.

Figure 7: Band diagram for 14 ALD cycles (~8 nm) ZnO/(i)aSi:H as deduced from the presented XPS data and band gaps from spectral ellipsometry. All values in eV. Values not directly obtained from photoelectron spectroscopy are marked in grey.

D. Comparison to theory

Finally, we use the information summarized in Fig. 7 to compare our experimental results for the ZnO/a-Si:H band offset to theory. The charge neutrality level (CNL) concept is well-established for the calculation of band offsets in heterojunctions [21,22,23]. It assumes that the band line-up in a heterojunction is determined by the continuum of interface-induced gap states. However, for a-Si:H, and in amorphous solids in general, the usual method of calculating such (virtual) gap states based on the calculation of band structures is not applicable due to the absence of long range translational periodicity. We have argued previously [24] that instead, the charge neutrality level (CNL), i.e. the energy in the band gap where the character of the gap states changes from valence band-(donor-) to conduction band- (acceptor-)like, can be determined from the defect state density in the a-Si:H and gap. Briefly, we have reasoned that in an intrinsic a-Si:H film, E_F will move to a position where the net charge in defects – band tails and dangling bonds – is zero, i.e. the defects are neutral. We have therefore taken this "intrinsic" Fermi level of such an a-Si:H, whose gap state density was calculated according to Powell & Deane's defect pool model [25], as its CNL. In [24], we found a value of $(E_F - E_{V,aSiH}) \equiv (CNL_{aSiH} - E_{V,aSiH}) \approx 1.10...1.12$ eV for $E_{g,aSiH} = 1.7...1.75$ eV; the error in this procedure was estimated to be about 100 meV. Interestingly, this value for the a-Si:H CNL is also close to our present experimental result for $(E_F - E_{V,aSiH}) = 1.05$ eV (Figs. 6 & 7). Thus, it appears that the net charge present in the a-Si:H is negligible both before and after ZnO deposition. Note, that in a-Si:H the rechargeable defect states (dangling bonds) in the a-Si:H also lead to Fermi level pinning effects, similar to those caused by c-Si surface dangling bonds [26], but originating from a-Si:H *bulk* defects. The magnitude of the pinning effect can be estimated to be similar on c-Si surfaces and in thin a-Si:H films: 10 nm of a-Si:H with a bulk gap state density of 10^{18} cm^{-3} – a common value for state of the art films – have a projected defect density per surface area of 10^{10} states/cm², similar to state of the art a-Si:/c-Si or SiO$_2$/c-Si [27] interface state densities. Therefore, the Fermi level position in a-Si:H is similarly sensitive to changes in the overall charge balance upon film deposition as the one on c-Si surfaces: To move E_F by e.g. 100 meV, about 10^9 states/cm² have to be recharged.

For the charge neutrality level of ZnO, a value of $(CNL_{ZnO} - E_{V,aSiH}) = 3.04 \pm 0.21$ eV was calculated, based on an analysis of valence band offsets reported for a wide range of ZnO-based heterostructures [28]. Thus, the valence band offset is obtained as

$$\Delta E_V^{CNL} = (CNL_{ZnO} - E_{V,ZnO}) - (CNL_{aSiH} - E_{V,aSiH}) + \Delta = (3.04 \pm 0.21 - 1.11 \pm 0.1 + 0.72 \pm 0.1) \text{ eV} = 2.65 \pm 0.3 \text{ eV}, \tag{3}$$

where the experimental value reported above was taken for the interface dipole Δ. Within the calculated error margin, there is thus an excellent agreement of the calculated value for ΔE_V^{CNL} with the experimental result of $\Delta E_V = 2.71 \pm 0.15$ eV.

IV. SUMMARY AND CONCLUSIONS

To sum up, we have shown that valence band photoelectron spectroscopy using monochromatized XPS (MXPS) is a powerful tool to investigate the initial growth stages of heterojunctions, and to determine the band offset in such junctions with a minimum of assumptions. We have developed a new approach to analyzing these data, where the XPS valence band spectra of ALD ZnO/a-Si:H heterojunctions are described as the superposition of scaled and shifted a-Si:H and ZnO bulk spectra.

As compared to the classical method, where core level positions are referenced to the valence band edges of bulk materials and shifts of these core level positions are considered to determine the band offset and changes in band bending, we believe that our approach has two main advantages: Firstly, comparing directly the valence band spectra requires less measurements, since there is no need to measure the core level peaks. This might also be beneficial e.g. for samples that degrade under prolonged X-ray irradiation, such as organic semiconductors. Secondly, as exemplified above in the comparison of O 1s vs. Zn 2p/3d core level shifts with increasing ZnO thickness, the assumption of constant core level-to-valence band edge is generally not expected to hold for non-abrupt interfaces. Thus, a careful and error-prone examination of core level and valence band spectra is required for the "classical" method. The determination of ΔE_V and band bending directly from valence band spectra does not suffer from these problems.

The intensity ratios of the a-Si:H and ZnO contributions to the valence band sum spectrum as obtained

with our new approach yield a growth rate of ~1 nm ZnO per ALD cycle. The relative shift of the spectra, together with a determination of the valence band edges of the bulk films from MXPS, allows to determine the valence band offset, which amounts to $\Delta E_V = 2.71 \pm 0.15$ eV in our samples. The concept of charge neutrality levels (CNLs) was successfully applied to calculate a theoretical value for ΔE_V: based on previously reported values of ZnO and a-Si:H CNLs [25,24] and our experimentally determined ZnO/a-Si:H interface dipole, a theoretical value of 2.65±0.3 eV is obtained, in excellent agreement with the experimental result.

Acknowledgements

References

[1] J. Müller, B. Rech, J. Springer, and M. Vanecek, Solar Energy **77**, 917 (2004).

[2] M. Berginski, J.Hüpkes, M.Schulte, G.Schöpe, H.Stiebig, B.Rech, and M.Wuttig, J. Appl. Phys. **101**, 074903 (2007).

[3] R. Rößler, C. Leendertz, L. Korte, N. Mingirulli, and B. Rech, J. Appl. Phys. **113**, 144513 (2013).

[4] C. Becker, F. Ruske, T. Sontheimer, B. Gorka, U. Bloeck, S. Gall, and B. Rech, J. Appl. Phys. **106**, 084506 (2009).

[5] D. Amkreutz, J. Haschke, T. Häring, F. Ruske, and B. Rech, Sol. En. Mat. Sol. Cells **123**, 13 (2014).

[6] D. Gerlach, R. G. Wilks, D. Wippler, M. Wimmer, M. Lozac'h, R. Félix, A. Mück, M. Meier, S. Ueda, H. Yoshikawa, M. Gorgoi, K. Lips, B. Rech, M. Sumiya, J. Hüpkes, K. Kobayashi, and M. Bär, Appl. Phys. Lett. **103**, 023903 (2013).

[7] J.R. Waldrop, R.W. Grant, S.P. Kowalczyk, and E.A. Kraut, J. Vac. Sci. Technol. A **3**, 835 (1985).

[8] T.F. Schulze, H.N. Beushausen, C. Leendertz, A. Dobrich, B. Rech, and L. Korte, Appl. Phys. Lett. **96**, 252102 (2010).

[9] E. Janocha and C. Pettenkofer, Appl. Surf. Sci. **257**, 10031 (2011).

[10] E. Janocha, A. Hofmann, and C. Pettenkofer, Rad. Phys. & Chem. **93**, 72 (2013).

[11] U. Meier and C. Pettenkofer, Appl. Surf. Sci. **252**, 1139 (2005).

[12] L. Korte and M. Schmidt, J. Non-Cryst. Sol. **354**, 2138 (2008).

[13] L. Korte, PhD thesis, Philipps-Universität Marburg and Hahn-Meitner-Institut Berlin, 2006, online: http://archiv.ub.uni-marburg.de/diss/z2006/0518.

[14] D.A. Shirley, Phys. Rev. B **5**, 4709 (1972).

[15] S. Tougaard, J. Electron Spectrosc. Relat. Phenom. **178–179**, 128 (2010).

[16] G.E. Jellison, Jr. and F.A. Modine, Appl. Phys. Lett. **69**, 371 (1996).

[17] J. Leng, J. Opsal, H. Chu, M. Senko, and D. Aspnes, Thin Solid Films **313-314**, 132 (1998).

[18] A. Pflug, V. Sittinger, F. Ruske, B. Szyszka, and G. Dittmar, Thin Solid Films **455-456**, 201 (2004).

[19] Z.C. Jin, I. Hamberg, and C. G. Granqvist, J. Appl. Phys. **64**, 5117 (1988).

[20] S. Ri, K. Hamano, and T. Nakagawa, J. Ceramic Assoc. Jap. **94,** 419 (1986).

[21] J. Tersoff, Phys. Rev. B **30**, 4874 (1984).

[22] F. Flores, A. Munoz, and J.C. Duran, Appl. Surf. Sci. **41-42**, 144 (1989).

[23] W. Mönch, J. Appl. Phys. **80**, 5076 (1996).

[24] L. Korte, T.F. Schulze, C. Leendertz, M. Schmidt, and B. Rech, MRS Symp Proc. **1321** (2011), doi: 10.1557/opl.2011.940.

[25] M. J. Powell & S. C. Deane, Phys. Rev. B **53**, 10121 (1996).

[26] F.J. Himpsel, G. Hollinger, R.A. Pollak, Phys. Rev. B **28**, 7014 (1983).

[27] W. Füssel, M. Schmidt, H. Angermann, G. Mende, H. Flietner, Nucl. Instrum. Methods Phys. Res. Sect. A **377**, 177 (1996).

[28] W. Mönch, Appl. Phys. Lett. **86**, 162101 (2005).